IEEE Photonics Journal
An IEEE Photonics Society Publication

Open Access

Environmentally Stable 1.56-μm Femtosecond Laser System With Discontinuous Selectable Repetition Rate

Volume 12, Number 2, April 2020

Hanmei Fu
Qiang Hao
Hang Gong
Peng Luo
Heping Zeng

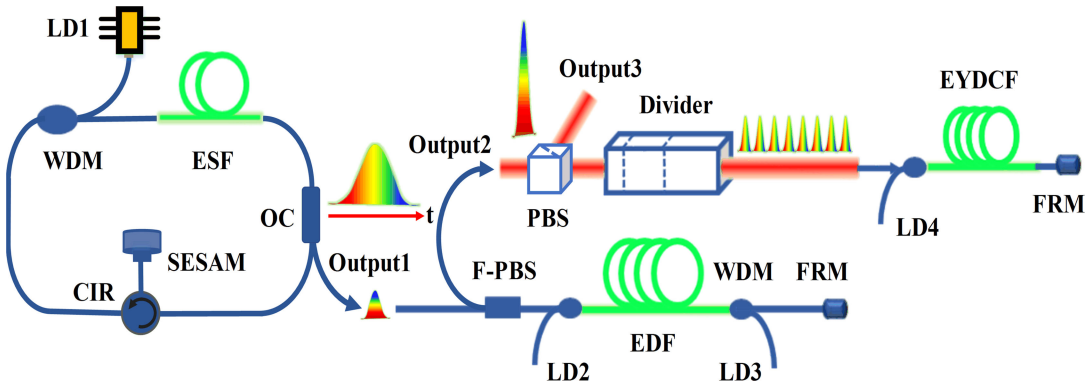

DOI: 10.1109/JPHOT.2020.2988419

Environmentally Stable 1.56-μm Femtosecond Laser System With Discontinuous Selectable Repetition Rate

Hanmei Fu,[1] Qiang Hao,[1] Hang Gong,[1] Peng Luo,[2] and Heping Zeng[3,4]

[1]Shanghai Key Laboratory of Modern Optical Systems and Engineering Research Center of Optical Instrument and Systems, Ministry of Education, School of Optical Electrical and Computer Engineering, University of Shanghai for Science and Technology, Shanghai 200093, China
[2]Guangdong Langyan Science and Technology Co., LTD, Dongguan 523000, China
[3]State Key Laboratory of Precision Spectroscopy, East China Normal University, Shanghai 200062, China
[4]Jinan Institute of Quantum Technology, Jinan 250101, China

DOI:10.1109/JPHOT.2020.2988419

Manuscript received February 15, 2020; revised April 9, 2020; accepted April 13, 2020. Date of publication April 20, 2020; date of current version May 26, 2020. This work was supported by the National Key Research and Development Program of China under Grant 2018YFB0407100. Corresponding author: Qiang Hao (e-mail: qianghao@usst.edu.cn).

Abstract: We demonstrate here an environmentally stable and compact Er-doped fiber laser system capable of delivering sub-100-fs pulse duration with discontinuous selectable repetition rate from 10 to 70 MHz. This laser source employs a SESAM harmonic mode-locked soliton laser to facilitate tunable repetition rate. A single-mode-fiber (SMF) amplifier and a double-cladding-fiber (DCF) amplifier (both with double-pass configuration) bridged by a three-stage YVO_4-based divider are used to manage the dispersion map and boost the seed pulses. With the help of $\times 8$ replicas, the seed pulses are simultaneously amplified and compressed with 90% recombining efficiency, generating 4.60-nJ pulse energy at 10 MHz and 6.13-nJ pulse energy at 70 MHz. The main advantage of the proposed laser system is that when pulse repetition rate is switched on-demand, the pulse duration can be kept almost unchanged only by simply adjusting the pump powers of the fiber amplifiers, instead of changing any optical device (the spacing between gratings or the length of fibers).

Index Terms: Mode-locked Laser, ultrafast laser, fiber amplifiers, tunable repetition rate.

1. Introduction

At the 1.55 μm eye-safe, optical telecommunication wavelength, Er-doped fiber lasers have become the most widely used laser sources [1]–[3]. Great efforts have been made to produce ultrashort pulse duration while promoting high laser power or pulse energy. Sometimes, femtosecond laser pulse with variable repetition rate is highly demanded for several applications, such as precision metrology, all-optical sampling, gas sensor system, pump-probe experiment, and waveguide writing [4]–[7]. Furthermore, pulse repetition rate is also expected to be easily tuned to reduce thermal accumulation [8]. In general, methods for adjusting the pulse repetition rate can be summarized into three techniques, such as pulse picking, pulse tuning, and pulse multiplying. Firstly, pulse picking technique is mainly applied in high energy laser amplifier where the repetition

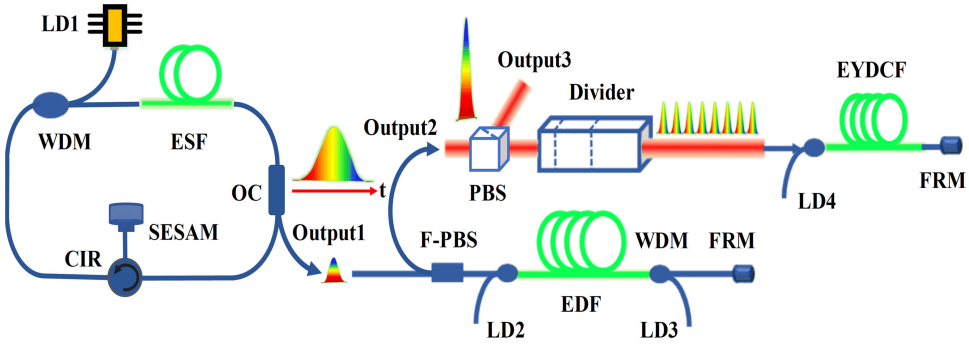

Fig. 1. Setup of the Er-doped fiber laser system. LD1, LD2, and LD3: 976-nm single-mode fiber-coupled laser diodes with the maximum pump power of 400 mW. ESF: Er-doped single-mode fiber with anomalous dispersion. OC: Output coupler. CIR: Circulator. SESAM: Fiber-coupled semiconductor saturable absorber mirror (SAM-1550-33-2ps, Batop). WDM: 980/1550 nm wavelength division multiplexer. F-PBS: Fiber-coupled polarization beam splitter. EDF: Er-doped fiber with normal dispersion. FRM: Faraday rotation mirror. PBS: Polarization beam splitter cube. Divider: Three-stage YVO_4-based divider. LD4: 976-nm multimode fiber-coupled laser diode with the maximum pump power of 9 W. EYDCF: 12/130 Er/Yb co-doped double-cladding fiber.

rate proportionally reduces from megahertz to kilohertz with the help of an extra-cavity AOM or EOM [8], [9]. Secondly, the so-called pulse tuning means that the repetition rate is continuously tunable near its fundamental repetition rate. The mainstream method for pulse tuning employs a stepping motor or a piezo-electric transducer (PZT) to change the optical length of a laser cavity. Reference [5] achieves a pulse tuning range of about 1.1 MHz by applying optical delay lines in the linear arm of a sigma cavity, while Ref. [10] achieves pulse tuning range of kHz by applying PZTs with nanometer accuracy. Most often, pulse tuning is used for repetition rate stabilization with an accuracy in the order of millihertz or even microhertz [11]. Thirdly, harmonic mode-locking (HML) is the mainstream technology for pulse multiplying. By controlling the pump power, intracavity dispersion, or polarization evolution, multiple ultrashort pulses can coexist in one round trip in the laser cavity while maintaining equal intervals [12]–[15].

Femtosecond pulse fiber amplifiers need build-in dispersion management, such as active/passive dispersion compensation fibers, chirped fiber Bragg gratings, bulk gratings or prisms [5], [8], [16]. In order to achieve the desired pulse duration with enough pulse energy, the group delay dispersion (GDD) mainly determined by the fiber length or the separation distance of bulk optics needs to be optimized according to the required pulse repetition rate. This greatly increases the complexity and instability of the ultrafast fiber laser system. In this letter, we report an environmentally stable and compact Er-doped fiber laser system operating in pulse multiplying mode. As the pulse repetition rate of the laser system is switched from 10 to 70 MHz, its pulse energy can be kept around 5 nJ with as short as 95-fs pulse duration. No optical hardware needs to be changed in this process except for optimizing the pump powers of the fiber amplifiers.

2. Experimental Setup and Results

The proposed laser system is comprised of a SESAM harmonic mode-locked laser oscillator and two-stage dispersion-managed fiber amplifiers (shown in Fig. 1). A sigma cavity is applied in our HML oscillator because of its excellent performances, such as high-grade stability, reliability and compactness [17]. It consists of 1.5-m Er-doped single-mode fiber (ESF) and 18.5-m SMF, corresponding to a fundamental repetition rate of $\sim$10 MHz. The group velocity dispersion (GVD) at 1.55 μm is -20.5 fs^2/mm for ESF and -21.6 fs^2/mm for SMF, respectively, yielding a net cavity dispersion of -0.43 ps^2. A laser diode (LD1) with a maximum pump power of 400 mW at 976 nm is used as the pump source, which is coupled into the ESF via a wavelength division multiplexer

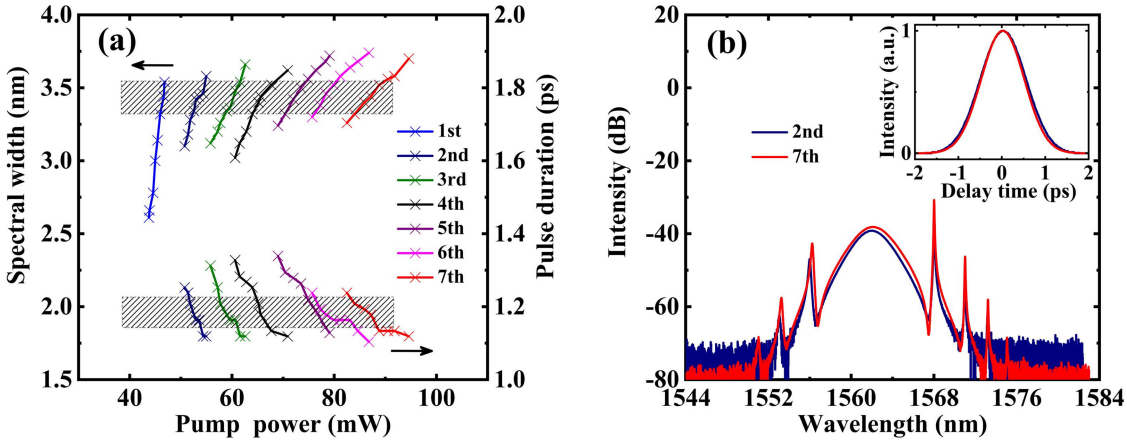

Fig. 2. (a) Spectral width (upper curves) and pulse duration (lower curves) of each harmonic as functions of the pump power. (b) Spectral and temporal traces of the 2nd and 7th harmonics.

(WDM). An output coupler (OC) with 70/30 ratio is used to extract output laser from the 30% port. All fibers in the oscillator are polarization-maintaining (PM) fibers, ensuring the immunity to environmental disturbances.

To achieve a pulse multiplying laser system, the characteristics of the harmonic mode-locked soliton laser are firstly investigated. In soliton regime where the laser oscillator is constructed by all anomalous dispersion fibers, the intracavity pulse energy is primarily determined by gain and dispersion. Therefore, an increase in the pump power will promote soliton bound or harmonic operation [18]. In our previous experiment, stable 1st to 10th harmonic (without pulse dropout) with a fundamental repetition rate of 39 MHz are observed in the SESAM cavity [17]. Interestingly, such a laser cavity experiences the process of soliton interaction for several seconds when switching between different harmonic orders. As shown in Fig. 2, the spectrum and the autocorrelation trace of each harmonic are recorded by a spectrum analyzer and a pulse autocorrelator, respectively. In our experiment, solitons with 10-MHz fundamental repetition rate are achieved at 44.6-mW pump power. As the pump power varies from 43.8 to 46.8 mW, the soliton remains stable (without mode jump) and its spectral width increases from 2.61 to 3.54 nm [see the upper curves in Fig. 2(a)]. Owing to the low output power at output1 which is less than the detection limit of the autocorrelator, the autocorrelation trace of soliton at fundamental repetition rate is hardly obtained.

In addition, the pump power thresholds of 2nd, 3rd, 4th, 5th, 6th, and 7th are measured to be 50.7, 55.2, 62.8, 71.0, 79.3, and 87.0 mW, successively. Taking the 2nd harmonic for example, as the pump power changes from 50.7 to 55.0 mW, the spectral width of pulse increases from 3.10 to 3.58 nm while the pulse duration decreases from 1.25 to 1.12 ps. By properly controlling the pump power, the spectral width as well as the pulse duration of high-order harmonics could match well with that of low-order harmonics. As shown in the shadow regions of Fig. 2(a), spectral width from 3.30 to 3.54 nm with the corresponding pulse duration from 1.21 to 1.16 ps could be achieved at each harmonic. This characteristic is helpful to simplify the subsequent fiber amplifiers and pulse compressor. Figure 2(b) and its inset compare the optical spectra and autocorrelation traces of the 2nd and 7th harmonics, respectively. It could be seen that the spectral and temporal traces of different harmonics keep nearly unchanged and the time-bandwidth products (TBP) maintain at $\sim$0.49. In order to avoid optical damage on the SESAM, the pump power is kept below 100 mW, and the available highest harmonic is 7th soliton.

Secondly, a dispersion-managed double-pass SMF pre-amplifier is applied to up-chirp and pre-amplify each harmonic [19]. Such an up-chirping can produce pulses with appropriate peak power and average power so as to mitigate the nonlinear effects and suppress the amplified spontaneous emission (ASE) in the subsequent main-amplifier. In our experiment, the fibers in pre-amplifier are

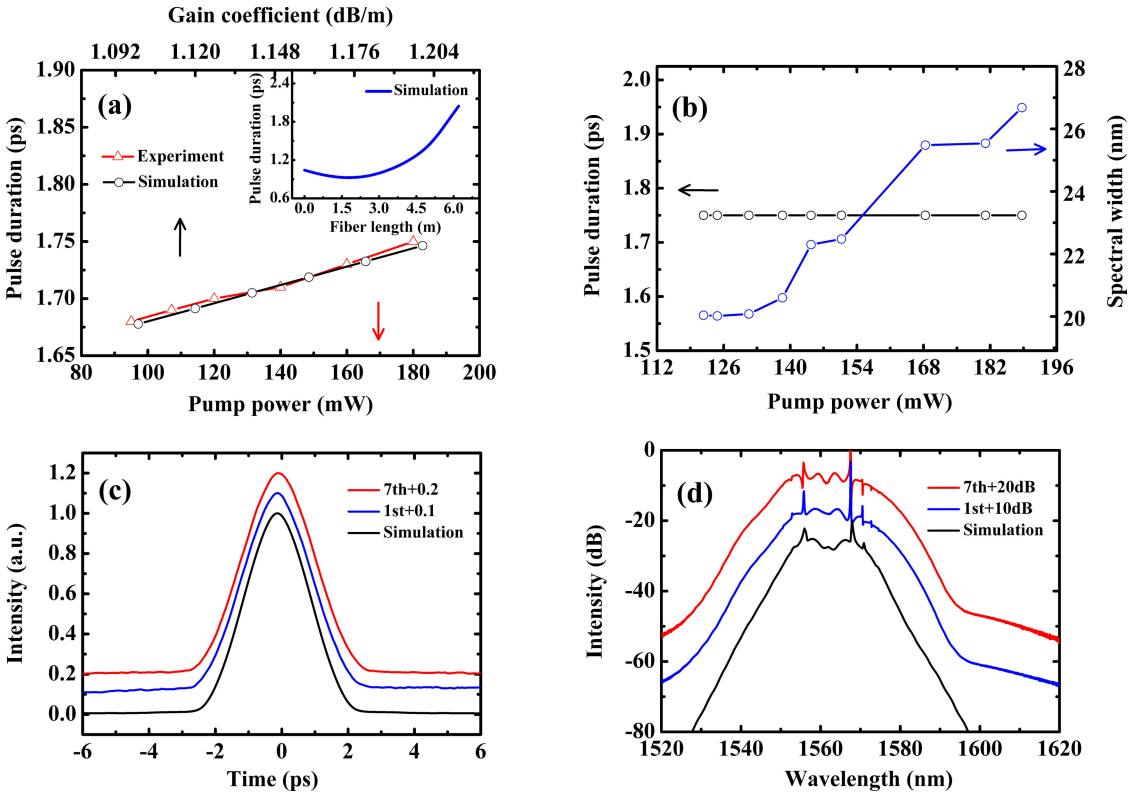

Fig. 3. (a) Experimental (red triangle line) and simulated (black circle line) pulse duration of pre-amplified pulse at 10-MHz repetition rate. Inset: Simulation result of pulse duration as function of the fiber length. (b) Pulse duration (black circle line) and spectral width (blue circle line) as functions of the total pump power at 10-MHz repetition rate. (c) Experimental results (red curve: the 7th harmonic, blue curve: the 1st harmonic) and simulation result (black curve) of pulse autocorrelation traces. (d) Experimental results (red curve: the 7th harmonic, blue curve: the 1st harmonic) and simulation result (black curve) of pulse spectra.

1.65-m EDF ($\beta_2 = 61.2$ fs^2/mm) and 1.40-m SMF. In order to investigate pulse evolution in the dispersion-managed pre-amplifier, the generalized nonlinear Schrödinger equation (GNLSE) with the split-step Fourier method is applied [20]. By using the spectral curve in Fig. 2(b), pulse with 1.04-ps temporal duration, 3.10-nm spectral width (corresponding to -0.12 ps^2 GDD pre-chirping on 825 fs transform-limited pulse), and 0.1-nJ pulse energy is applied as the seed laser. A 6.20-m-long active fiber with GVD of 23 fs^2/mm and nonlinear coefficient of 4.0 W^{-1}·km^{-1} performs the simulation. It is worth noting that EDF provides positive GVD as well as gain and SMF provides negative GVD in the experiment, while the dispersion and gain are uniformly distributed on the fiber in simulation.

In the pre-amplifier, the negatively chirped input pulse is firstly temporally compressed and then broadened owing to the effects of positive GVD and SPM. The inset in Fig. 3(a) shows the simulation result of the pulse duration in the pre-amplifier when the gain coefficient of active fiber is 1.6 dB/m. In details, the 1.04-ps pulse is compressed to 910 fs along the 1.80-m fiber length and then stretched to 2.03 ps at 6.20-m fiber length. By comparing the average output powers in the experimental and simulation results, we obtain the relationship between the pump power and the gain coefficient. The pulse duration at 6.20-m fiber length is recorded in Fig. 3(a) as the gain coefficient (as well as the pump power) is changed. As the pump power of LD2 increases from 95 to 180 mW, both experimental (red triangle line) and simulated (black circle line) pulse duration of the pre-amplified pulse increase linearly. The pulse duration is 1.68 ps when the pump power is 95 mW,

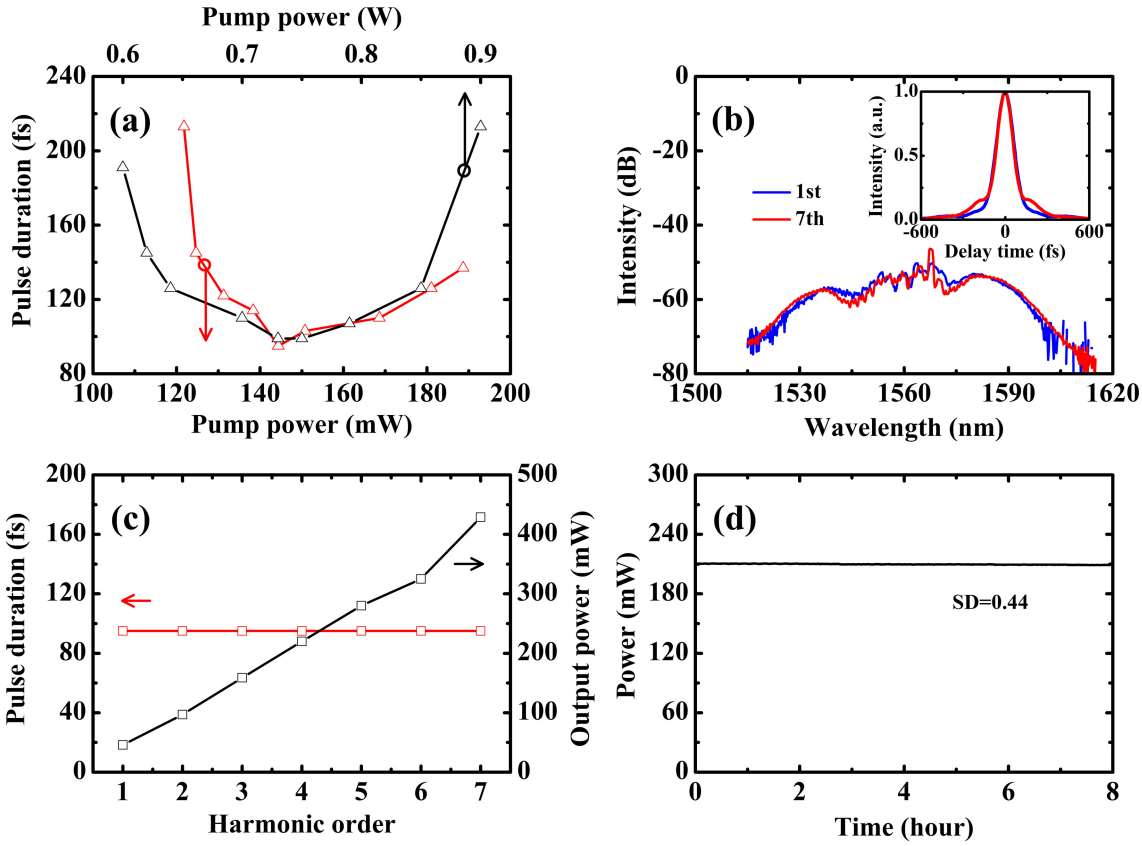

Fig. 4. (a) The available pulse duration at output3 by optimizing the pump power of the pre-amplifier (red triangle line) and the main-amplifier (black triangle line) at 10-MHz repetition rate, respectively. (b) Spectral and temporal traces of the 1st and 7th harmonics at output3. (c) Pulse duration (red square line) and output power (black square line) of each harmonic in the main-amplifier. (d) Power stability of the main-amplifier at the 4th harmonic.

and it increases to 1.75 ps when the pump power increases to 180 mW. Obviously, the change of pulse duration in fact could agree well with that of simulation, and the corresponding mean absolute percentage error (MAPE) of two curves is calculated to be about 0.23%. From experimental point of view, what is worthy to note that by further applying forward (LD2) and backward (LD3) pump configuration, the nonlinear evolution process (especially the chirp of the pre-amplified pulse) could be finely controlled. A double-pass configuration with the combination of a F-PBS and a FRM is used to cancel the environmental influence on the non-PM fiber in the pre-amplifier. The black circle line in Fig. 3(b) shows that the pulse duration can keep constant at 1.75 ps within the pump power from 122.5 to 189.5 mW (the total pump power of LD2 and LD3), while the corresponding spectral width increases from 19.8 to 27.0 nm (see the blue circle line). This characteristic is helpful to finely manage the pulse chirping in the pre-amplifier as well as the pulse evolution in the subsequent main-amplifier where the pulse is being amplified and simultaneously compressed, especially when the seed laser is switched to another harmonic. As results, Figs. 3(c) and 3(d) show the pulse characteristics of experimental (the 1st and 7th harmonics) and simulation results (single pulse) in the pre-amplifier. The temporal and spectral shapes of the pre-amplified pulse can be kept the same at different harmonics by controlling the gain of the pre-amplifier.

Thirdly, a three-stage YVO_4-based divider with lengths of 10, 20, and 40 mm followed by a double-pass DCF main-amplifier is used to produce $\times 8$ identical replicas and further boost the pulses, respectively [19], [21]. The first and third YVO_4 crystals (from left to right) have their crystal

optical axes (OA) oriented at an angle of 45° to the horizontal plane, while the second YVO_4 crystal axis is oriented in the horizontal plane. Therefore, the pulse with horizontal polarization transmitted from PBS is split into two replicas, but with perpendicular polarization. Subsequently, eight replicas are produced by the second and third YVO_4 crystals. In the main-amplifier, a length of 1.20-m EYDCF with anomalous dispersion acts as the gain fiber to simultaneously amplify and compress the replicas [22]. It is found that once the dispersion map is roughly managed, the pulse duration at output3 could be optimized to its shortest value by finely adjusting the pump powers of LD2, LD3, and LD4. Figure 4(a) indicates that there exists an optimal position of pump power which can support $<$100 fs pedestal-free pulse at 10-MHz repetition rate. The red triangle line and black triangle line represent the evolution of pulse duration of the amplified pulse when the pump powers of pre-amplifier and main-amplifier are tuned respectively. The shortest pulse is achieved at 144-mW pump power for the pre-amplifier (keeping LD4 $=$ 0.73 W) and 0.73-W pump power for the main-amplifier (keeping the total pump power of LD2 and LD3 $=$ 144 mW), as shown in Fig. 4(a). Deviating from the optimal pump power would both stretch the pulse duration.

By optimizing the pump powers of the pre-/main-amplifiers, the pulse characteristics could keep unchanged as the repetition rate of seed laser is switched on-demand. As can be seen in Fig. 4(b) and its inset, the output spectrum and autocorrelation trace of the 1st harmonic match well with that of the 7th harmonic. Nevertheless, a little pulse pedestal could be observed. The red square line in Fig. 4(c) indicates that pulses of each harmonic could be indistinguishably compressed to 95 fs as the average power increases linearly with harmonic order (black square line). Figure 4(d) shows the output power stability of the main-amplifier operating at the 4th harmonic over 8 hours. Owing to the environmentally stable laser architecture, as low as 0.82% of power fluctuation is achieved, and the corresponding standard deviation (SD) is calculated to be 0.44.

3. Conclusion

In conclusion, we propose a HML oscillator and cascaded dispersion-managed double-pass fiber amplifiers for ultrashort pulse generation with $\sim$5-nJ energy and $<$100-fs duration from 10- to 70-MHz repetition rate. As the pulse repetition rate is switched on-demand, the pulse duration and spectrum can keep nearly unchanged only by adjusting the pump powers of the amplifiers, instead of changing any optical device. This method paves a new way for the generation of high energy femtosecond pulse at 1.55 μm. Besides, in many cases, the property of switchable pulse repetition rate while keeping other parameters constant is highly desirable [23].

References

[1] M. F. Ferreira, M. V. Facão, S. V. Latas, and M. H. Sousa, "Optical Solitons in Fibers for Communication Systems," *Fiber and Integrated Opt.*, vol. 24, pp. 287–313, May 2005.
[2] T. R. Schibli *et al.*, "Frequency metrology with a turnkey all-fiber system," *Opt. Lett.*, vol. 29, pp. 2467–2469, Nov. 2004.
[3] F. Morin, F. Druon, M. Hanna, and P. Georges, "Microjoule femtosecond fiber laser at 1.6 μm for corneal surgery applications," *Opt. Lett.*, vol. 34, pp. 1991–1993, Jul. 2009.
[4] Y. S. Liu, J. G. Zhang, G. F. Chen, W. Zhao, and J. Bai, "Low-timing-jitter, stretched-pulse passively mode-locked fiber laser with tunable repetition rate and high operation stability," *J. Opt.*, vol. 12, Sep. 2010, Art. no. 095204.
[5] H. Hundertmark, D. Kracht, M. Engelbrecht, D. Wandt, and C. Fallnich, "Stable sub-85 fs passively mode-locked Erbium-fiber oscillator with tunable repetition rate," *Opt. Express*, vol. 12, pp. 3178–3183, Jul. 2004.
[6] Y. Zhang *et al.*, "Novel Intracavity Sensing Network Based on Mode-Locked Fiber Laser," *IEEE Photon. Tech. Lett.*, vol. 14, pp. 1336–1338, Sep. 2002.
[7] L. Shah, A. Y. Arai, S. M. Eaton, and P. R. Herman, "Waveguide writing in fused silica with a femtosecond fiber laser at 522 nm and 1 MHz repetition rate," *Opt. Express*, vol. 13, pp. 1999–2006, Mar. 2005.
[8] R. Huber, F. Adler, A. Leitenstorfer, M. Beutter, P. Baum, and E. Riedle, "12-fs pulses from a continuous-wave-pumped 200-nJ Ti:sapphire amplifier at a variable repetition rate as high as 4 MHz," *Opt. Lett.*, vol. 28, pp. 2118–2120, Nov. 2003.
[9] F. Kienle *et al.*, "High-power, variable repetition rate, picosecond optical parametric oscillator pumped by an amplified gain-switched diode," *Opt. Express*, vol. 18, pp. 7602–7610, Apr. 2010.
[10] G. R. Lin, Y. C. Chang, T. A. Liu, and C. L. Pan, "Piezoelectric-transducer-based optoelectronic frequency synchronizer for control of pulse delay in a femtosecond passively mode-locked Ti: sapphire laser," *Appl. Opt.*, vol. 42, pp. 2843–2848, May 2003.

[11] Y. Feng *et al.*, "Environmental-adaptability analysis of an all polarization-maintaining fiber-based optical frequency comb," *Opt. Express*, vol. 23, pp. 17549–17559, Jun. 2015.
[12] A. B. Grudinin and S. Gray, "Passive harmonic mode locking in soliton fiber lasers," *J. Opt. Soc. Am. B*, vol. 14, pp. 144–154, Jan. 1997.
[13] N. Haverkamp, H. Hundertmark, C. Fallnich, and H. R. Telle, "Frequency stabilization of mode-locked Erbium fiber lasers using pump power control," *Appl. Phys. B*, vol. 78, pp. 321–324, Feb. 2004.
[14] J. Sotor, G. Sobon, K. Krzempek, and K. M. Abramski, "Fundamental and harmonic mode-locking in erbium-doped fiber laser based on graphene saturable absorber," *Opt. Communications*, vol. 285, pp. 3174–3178, Mar. 2012.
[15] Z. X. Zhang, L. Zhan, X. X. Yang, S. Y. Luo, and Y. X. Xia, "Passive harmonically mode-locked erbium-doped fiber laser with scalable repetition rate up to 1.2 GHz," *Laser Phys. Lett.*, vol. 4, pp. 592–596, Feb. 2007.
[16] I. Morohashi, T. Sakamoto, H. Sotobayashi, T. Kawanishi, I. Hosako, and M. Tsuchiya, "Widely repetition-tunable 200 fs pulse source using a Mach–Zehnder-modulator-based flat comb generator and dispersion-flattened dispersion-decreasing fiber," *Opt. Lett.*, vol. 33, pp. 1192–1194, Jun. 2008.
[17] Q. Hao, Y. Wang, P. Luo, H. Hu, and H. Zeng, "Self-starting dropout-free harmonic mode-locked soliton fiber laser with a low timing jitter," *Opt. Lett.*, vol. 42, pp. 2330–2333, Jun. 2017.
[18] S. F. Lin, Y. H. Lin, C. H. Cheng, Y. C. Chi, and G. R. Lin, "Stability and Chirp of Tightly Bunched Solitons From Nonlinear Polarization Rotation Mode-Locked Erbium-Doped Fiber Lasers," *J. Lightwave Tech.*, vol. 34, pp. 5118–5128, Nov. 2016.
[19] Q. Hao *et al.*, "Divided-pulse nonlinear amplification and simultaneous compression," *Appl. Phys. Lett.*, vol. 106, Mar. 2015, Art. no. 101103.
[20] G. P. Agrawal, *Nonlinear Fiber Optics*, 5th ed. New York, NY, USA: Academic, 2013.
[21] Q. Hao, Y. Wang, T. Liu, H. Hu, and H. Zeng, "Divided-Pulse Nonlinear Amplification at 1.5 μm," *IEEE Photon. J.*, vol. 8, Oct. 2016, Art. no. 7101908.
[22] I. Pavlov, E. Ilbey, E. Dülgergil, A. Bayri, and F. Ö. Ilday, "High-power high-repetition-rate single-mode Er-Yb-doped fiber laser system," *Opt. Express*, vol. 20, pp. 9471–9475, Apr. 2012.
[23] P. E. Schrader, R. L. Farrow, D. A. V. Kliner, J. P. Fève, and N. Landru, "High-power fiber amplifier with widely tunable repetition rate, fixed pulse duration, and multiple output wavelengths," *Opt. Express*, vol. 14, pp. 11528–11538, Nov. 2006.